

Gyration-Radius Expansion Factor of Oligo- and Poly(α -methylstyrene)s in Dilute Solution

Masashi Osa, Yukiyoishi Ueno, Takenao Yoshizaki, and Hiromi Yamakawa*

Department of Polymer Chemistry, Kyoto University, Kyoto 606-8501, Japan

Received April 13, 2001; Revised Manuscript Received June 1, 2001

ABSTRACT: The mean-square radius of gyration $\langle S^2 \rangle$ was determined from small-angle X-ray scattering and light scattering measurements for atactic oligo- and poly(α -methylstyrene)s (a-P α MS) with the fraction of racemic diads $f_r = 0.72$ in toluene at 25.0 °C, in 4-*tert*-butyltoluene at 25.0 °C, and in *n*-butyl chloride at 25.0 °C in the range of weight-average molecular weight from 1.04×10^3 to 5.46×10^6 . The gyration-radius expansion factor α_S was then evaluated from the values of $\langle S^2 \rangle$ so determined along with those of $\langle S^2 \rangle_\Theta$ previously determined for the same samples in cyclohexane at 30.5 °C (Θ). It is shown that the plots of α_S against the scaled excluded-volume parameter \tilde{z} for a-P α MS along with those for atactic polystyrene (a-PS) and atactic and isotactic poly(methyl methacrylate)s previously studied form a single-composite curve, confirming the validity of the quasi-two-parameter scheme that all expansion factors are functions only of \tilde{z} irrespective of the differences in polymer species (chain stiffness and local chain conformation) and solvent condition. The excluded-volume strength for a-P α MS in good solvents is also discussed in comparison with that for a-PS.

Introduction

As the continuation of experimental work¹ on dilute solution behavior of flexible polymers and their oligomers in the unperturbed Θ state on the basis of the helical wormlike (HW) chain model,^{2,3} we recently made a start in the study of atactic poly(α -methylstyrene) (a-P α MS)^{4–6} with the fraction of racemic diads $f_r = 0.72$.⁷ Following the well-established procedures by means of the HW theory,^{2,3} the data for the mean-square radius of gyration⁴ $\langle S^2 \rangle_\Theta$, scattering function,⁵ intrinsic viscosity⁶ $[\eta]_\Theta$, and translational diffusion coefficient⁶ D_Θ in cyclohexane at 30.5 °C (Θ) were analyzed to show that the a-P α MS chain has rather large chain stiffness and strong helical nature like the atactic poly(methyl methacrylate) (a-PMMA) chain with $f_r = 0.79$.^{2,8} We note that by the term “helical nature” we mean that the chain tends to retain large and clearly distinguishable helical portions in dilute solution.² It was then confirmed that this feature is characteristic of disubstituted asymmetric polymers with large f_r such as the above ones (a-P α MS with $f_r = 0.72$ and a-PMMA with $f_r = 0.79$) for which the two successive skeletal bond angles are appreciably different from each other with the predominance of the trans–trans conformation.^{2,9} The disagreement between our and literature^{10–16} data for $\langle S^2 \rangle_\Theta$, $[\eta]_\Theta$, and D_Θ for a-P α MS in the range of large molecular weight M was also discussed in detail.^{4,6}

Now, with the above results of molecular characterization for the unperturbed a-P α MS chain, we proceed to investigate the excluded-volume problems for a-P α MS in dilute solution, i.e., the gyration-, viscosity-, and hydrodynamic-radius expansion factors and also the second virial coefficient. In this paper as a first step, we consider the gyration-radius expansion factor α_S of a-P α MS and its oligomers. Within the framework of the HW theory, the expansion factors (intramolecular excluded-volume effect) may be described by the so-called quasi-two-parameter (QTP) theory,² which claims that they are functions only of the intramolecular scaled excluded-volume parameter \tilde{z} . The main purpose of this paper is then to verify the validity of the theory of α_S

for the a-P α MS chain with a strong helical nature. The source of inconsistency in our and literature data for these properties of a-P α MS is also discussed in the present and forthcoming papers.

The perturbed HW chain² enables us to take account of both effects of excluded volume and chain stiffness, leading to the above QTP prediction that all the expansion factors may be written in terms of \tilde{z} in place of the conventional excluded-volume parameter z in the two-parameter (TP) theory.¹⁷ The parameter \tilde{z} is related to z by the equation $\tilde{z} = \frac{3}{4}K(\lambda L)z$, where λL is the reduced total contour length of the HW chain defined as its total contour length L divided by the stiffness parameter λ^{-1} , and the function K of λL becomes $\frac{4}{3}$ and 0 in the limits of $\lambda L \rightarrow \infty$ and 0, respectively, so that the QTP theory becomes identical with the TP theory in the former (random coil) limit. In the latter (rigid rod or short chain) limit, all the expansion factors become unity and the intramolecular excluded-volume effect vanishes. We note that, in general, neither the TP nor the QTP scheme is valid for the second virial coefficient (intermolecular excluded-volume effect).

To verify experimentally the validity of the QTP prediction for α_S mentioned above, the mean-square radius of gyration $\langle S^2 \rangle$ must be determined in several good solvents for a-P α MS test samples over a wide range of M , including the oligomer region, for which $\langle S^2 \rangle_\Theta$ in cyclohexane at 30.5 °C (Θ) have already been determined. Thus, we determine $\langle S^2 \rangle$ in the range of weight-average molecular weight M_w from 1.04×10^3 to 5.46×10^6 in toluene, 4-*tert*-butyltoluene, and *n*-butyl chloride at 25.0 °C.

Experimental Section

Materials. All the a-P α MS samples except the one (AMS550) with the highest M_w used in this work are the same as those used in the previous study of $\langle S^2 \rangle_\Theta$ in cyclohexane at 30.5 °C (Θ),⁴ i.e., fractions separated by preparative gel permeation chromatography (GPC) or fractional precipitation from the original samples prepared by living anionic polymerization.⁷ We note that the sample AMS40 is a fraction from the commercial sample 20538-2 from Polymer Laboratories Ltd.

Table 1. Values of M_w , x_w , M_w/M_n , and f_i for Atactic Oligo- and Poly(α -methylstyrene)s

sample	M_w	x_w	M_w/M_n	f_i
OAMS8 ^a	1.04×10^3	8.29	1.01	
OAMS10	1.27×10^3	10.3	1.01	
OAMS13	1.60×10^3	13.1	1.02	0.71
OAMS25	2.96×10^3	24.6	1.06	0.72
OAMS33	3.95×10^3	33.0	1.04	0.72
OAMS67	7.97×10^3	67.1	1.04	0.72
AMS1	1.30×10^4	109	1.02	0.73
AMS2	2.48×10^4	209	1.02	0.73
AMS5	5.22×10^4	442	1.02	0.73
AMS24	2.38×10^5	2010	1.05	0.73
AMS40	4.07×10^5	3450	1.02	0.73
AMS80	8.50×10^5	7200	1.05	0.72
AMS200	2.06×10^6	17400	1.05	0.72
AMS320	3.22×10^6	27300	1.05	0.73
AMS550	5.46×10^6	46300		0.70

^a The results for OAMS8 through AMS320 (except for M_w/M_n for AMS320) have been reproduced from Table 1 of ref 4.

We also used an additional sample AMS550 separated by fractional precipitation from an original sample prepared by the same method as that for the other original samples^{4,7} at the initial monomer concentration $[M]_0 = 1.1$ mol/L and polymerization temperature $T_p = -40$ °C. We note that we adopted the value 1.1 mol/L as $[M]_0$, which is larger than the value 0.6 mol/L adopted for the preparation of the other original samples, to obtain the original sample with very large M_w . We also note that the initiating chain end of each polymerized sample is a *sec*-butyl group, and the other end is a hydrogen atom.

The values of M_w determined from light scattering (LS) measurements (in cyclohexane at 30.5 °C), the weight-average degree of polymerization x_w estimated from M_w , the ratio of M_w to the number-average molecular weight M_n determined by analytical GPC, and f_i determined from ¹H and/or ¹³C NMR spectra are given in Table 1. The first (OAMS8) through 14th (AMS320) rows except for the M_w/M_n value in the 14th row have been reproduced from Table 1 of ref 4. The values of M_w and f_i of AMS550 were determined in this work (see succeeding subsections). Although f_i of the samples OAMS8 and OAMS10 could not be determined because of the complexity of their ¹H NMR spectra, they may be regarded as having almost the same value of f_i as OAMS13, since the samples OAMS8, OAMS10, and OAMS13 are fractions from one original sample.⁷ As seen from the values of f_i , all the samples except AMS550 have the fixed stereochemical composition $f_i = 0.72 \pm 0.01$. The value of f_i of AMS550 is somewhat smaller than those for the others. This may be regarded as arising from the fact that the value of $[M]_0$ adopted for the preparation of AMS550 is larger than those for the other samples. As seen from the values of M_w/M_n , all the samples except AMS550 are very narrow in molecular weight distribution. Although the value of M_w/M_n for the sample AMS550 could not be determined with high accuracy because of the lack of the GPC calibration curve in the necessary range, its molecular weight distribution may be considered to be as narrow as that of the other samples.

The solvents cyclohexane, toluene, and *n*-butyl chloride were purified according to standard procedures. The solvent 4-*tert*-butyltoluene was purified by distillation under reduced pressure in a dried nitrogen atmosphere after refluxing over sodium.

¹H NMR. A ¹H NMR spectrum was recorded for AMS550 on a JEOL JMN GX-400 spectrometer at 399.8 MHz. It was taken in deuterated chloroform at 50 °C using an rf pulse angle of 90° with a pulse repetition time of 15 s. As in the previous paper,⁷ we determined the value of f_i of AMS550 from the ¹H NMR spectrum by the use of the assignments of the proton signals proposed by Brownstein et al.¹⁸ The f_i value so determined is given in the last row in the last column of Table 1.

Light Scattering. LS measurements were carried out to determine M_w and $\langle S^2 \rangle_\Theta$ for AMS550 in cyclohexane at 30.5

°C (Θ). Measurements were also carried out to determine M_w and $\langle S^2 \rangle$ in toluene, 4-*tert*-butyltoluene, and *n*-butyl chloride at 25.0 °C for the samples AMS24 through AMS550.

A Fica 50 light-scattering photometer was used for all the measurements with vertically polarized incident light of wavelength 436 nm. For a calibration of the apparatus, the intensity of light scattered from pure benzene was measured at 25.0 °C at a scattering angle of 90°, where the Rayleigh ratio $R_{90}(90^\circ)$ of pure benzene was taken as $46.5 \times 10^{-6} \text{ cm}^{-1}$.¹⁹ The depolarization ratio ρ_u of pure benzene at 25.0 °C was determined to be 0.41 ± 0.01 . Scattered intensities were measured at five or six different concentrations and at scattering angles ranging from 15.0° to 150°. The data obtained were treated by using the Berry square-root plot.²⁰ For all the samples AMS24 through AMS550 in all the solvents, corrections for the optical anisotropy were unnecessary.

The most concentrated solutions of the samples were prepared gravimetrically and made homogeneous by continuous stirring in the dark at ca. 50 °C for 7 days in cyclohexane and at room temperature for 1–3 days in the good solvents. The solutions were optically purified by filtration through a Teflon membrane of pore size 0.45 or 1.0 μm. The solutions of lower concentrations were obtained by successive dilution. The weight concentrations of the test solutions were converted to the polymer mass concentrations c by the use of the densities of the respective solutions calculated with the partial specific volumes v_2 of the samples and with the density ρ_0 of the solvents. The quantities v_2 and ρ_0 were measured with a pycnometer of the Lipkin-Davison type having the volume of 10 cm³. The values of v_2 so determined for the samples AMS24 through AMS550 in toluene, 4-*tert*-butyltoluene, and *n*-butyl chloride at 25.0 °C are independent of M_w and are 0.875, 0.884, and 0.874 cm³/g, respectively. For AMS550 in cyclohexane at Θ, we used the value 0.885 cm³/g previously⁴ determined. The values of ρ_0 of toluene, 4-*tert*-butyltoluene, and *n*-butyl chloride at 25.0 °C are 0.8622, 0.8574, and 0.8810 g/cm³, respectively. For the value of ρ_0 of cyclohexane at Θ, we used the previous value 0.7683 g/cm³.⁴

The refractive index increment $\partial n/\partial c$ was measured at wavelength of 436 nm by the use of a Shimadzu differential refractometer. The values of $\partial n/\partial c$ determined for the samples AMS24 through AMS550 in toluene, 4-*tert*-butyltoluene, and *n*-butyl chloride at 25.0 °C are independent of M_w and are 0.131₀, 0.134₂, and 0.224₀ cm³/g, respectively. For AMS550 in cyclohexane at Θ, we used the value 0.203₇ cm³/g previously⁴ determined.

The value of the refractive index n_0 of 4-*tert*-butyltoluene at 25.0 °C measured at wavelength of 436 nm by the use of an Abbe refractometer (ERMA OPTICAL WORKS) is 1.507₆. For the values of n_0 of toluene and *n*-butyl chloride at 25.0 °C, we used the literature values²¹ 1.515₁ and 1.408₈, respectively. For the value of n_0 of cyclohexane at Θ, we used the value 1.429₈ previously⁴ adopted.

Small-Angle X-ray Scattering. Small-angle X-ray scattering (SAXS) measurements were carried out for the samples OAMS8 through AMS5 in toluene at 25.0 °C and for the samples OAMS13, OAMS67, and AMS2 in 4-*tert*-butyltoluene at 25.0 °C by the use of an Anton Paar Kratky U-slit camera with an incident X-ray of wavelength 1.54 Å (Cu Kα line). The apparatus system and the methods of data acquisition and analysis are the same as those described in a previous paper.²²

The measurements were performed for four or five solutions of different concentrations for each polymer sample and for the solvent at scattering angles ranging from 1×10^{-3} rad to a value at which the scattered intensity was negligibly small. Corrections for the stability of the X-ray source and the detector electronics were made by measuring the intensity scattered from Lupolene (a platelet of polyethylene) used as a working standard before and after each measurement for a given sample solution and the solvent. The effect of absorption of X-rays by a given solution or the solvent was also corrected by measuring the intensity scattered from Lupolene with insertion of the solution or solvent between the X-ray source and Lupolene. The degree of absorption increased linearly with increasing solute concentration.

Table 2. Results of SAXS and LS Measurements for Atactic Oligo- and Poly(α -methylstyrene)s in Θ and Good Solvents

sample	cyclohexane, 30.5 °C (Θ)		toluene, 25.0 °C		4- <i>tert</i> -butyltoluene, 25.0 °C		<i>n</i> -butyl chloride, 25.0 °C	
	$10^{-4}M_w$	$\langle S^2 \rangle^{1/2}$, Å	$10^{-4}M_w$	$\langle S^2 \rangle^{1/2}$, Å	$10^{-4}M_w$	$\langle S^2 \rangle^{1/2}$, Å	$10^{-4}M_w$	$\langle S^2 \rangle^{1/2}$, Å
OAMS8				6.3 ₀				
OAMS10				7.5 ₃				
OAMS13				9.1 ₈		9.1 ₂		
OAMS25				$1.3_9 \times 10$				
OAMS33				$1.6_4 \times 10$				
OAMS67				$2.4_4 \times 10$		$2.3_8 \times 10$		
AMS1				$3.2_2 \times 10$				
AMS2				$4.5_9 \times 10$		$4.3_0 \times 10$		
AMS5				$7.2_2 \times 10$				
AMS24			24.3	$1.7_5 \times 10^2$	23.7	$1.4_7 \times 10^2$	24.3	$1.4_3 \times 10^2$
AMS40			40.7	$2.4_2 \times 10^2$	40.8	$1.9_5 \times 10^2$	41.0	$1.9_2 \times 10^2$
AMS80			87.7	$3.7_6 \times 10^2$	86.2	$3.0_0 \times 10^2$	85.3	$2.8_7 \times 10^2$
AMS200			203	$6.2_9 \times 10^2$	200	$4.9_6 \times 10^2$	204	$4.7_6 \times 10^2$
AMS320			324	$8.2_9 \times 10^2$	316	$6.5_1 \times 10^2$	320	$6.1_0 \times 10^2$
AMS550	546	$6.0_9 \times 10^2$	556	$1.1_4 \times 10^3$	556	$8.9_7 \times 10^2$	547	$8.2_5 \times 10^2$

The excess reduced scattered intensity $\Delta I_R(k)$ as a function of the magnitude k of the scattering vector was determined from the observed (smeared) excess reduced intensity by the modified Glatter desmearing method, which consists of expressing the true scattering function in terms of cubic B-spline functions, as described before.²² Here, k is given by

$$k = (4\pi/\lambda_0) \sin(\theta/2) \quad (1)$$

with λ_0 the wavelength of the incident X-ray and θ the scattering angle. Then the data for $\Delta I_R(k)$ were analyzed by using the Berry square-root plot²⁰ to evaluate the apparent mean-square radius of gyration $\langle S^2 \rangle_s$.

The test solutions of each sample were prepared in the same manner as that in the case of LS measurements. The values of v_2 necessary for the evaluation of c for the test solutions were determined in the same manner as that mentioned in the last subsection. The values of v_2 in toluene at 25.0 °C are 0.934, 0.916, 0.904, 0.899, 0.898, 0.886, and 0.882 cm³/g for the samples OAMS8 through AMS1, respectively, and 0.875 cm³/g for the samples AMS2 and AMS5. The values of v_2 for the samples OAMS13, OAMS67, and AMS2 in 4-*tert*-butyltoluene at 25.0 °C are 0.917, 0.898, and 0.884 cm³/g, respectively.

Results

The values of the apparent root-mean-square radius of gyration $\langle S^2 \rangle_s^{1/2}$ determined from SAXS measurements for the samples OAMS8 through AMS5 in toluene at 25.0 °C are 7.0₉, 8.2₁, 9.7₄, 14.2, 16.7, 24.6, 32.3, 46.0, and 72.2 Å, respectively, and those for the samples OAMS13, OAMS67, and AMS2 in 4-*tert*-butyltoluene at 25.0 °C are 9.6₉, 24.1, and 43.2 Å, respectively. We note that the transmittance of the solvent *n*-butyl chloride was so small that SAXS measurements could not be performed in it. As done in the previous study of $\langle S^2 \rangle_\Theta$ of a-PaMS in cyclohexane at 30.5 °C (Θ),⁴ the (true) root-mean-square radius of gyration $\langle S^2 \rangle^{1/2}$ may be calculated from

$$\langle S^2 \rangle_s = \langle S^2 \rangle + S_c^2 \quad (2)$$

with the values of $\langle S^2 \rangle_s^{1/2}$ determined above, where S_c is the radius of gyration of the cross section of the distribution of the (excess) electrons around the chain contour. The values of S_c^2 in toluene at 25.0 °C and in 4-*tert*-butyltoluene at 25.0 °C have been estimated as usual^{2,4,22} from the asymptotic values of v_2 in the limit of $M_w \rightarrow \infty$ given in the Experimental Section, i.e., 0.875 and 0.884 cm³/g in the respective solvents at 25.0 °C, and the results are 10.6 and 10.7 Å², respectively. We

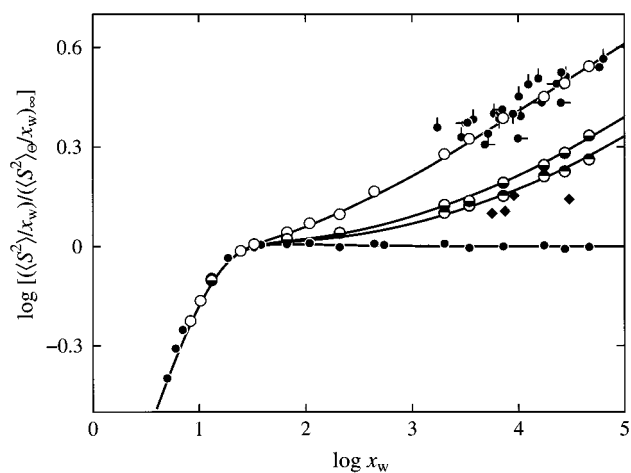


Figure 1. Double-logarithmic plots of $(\langle S^2 \rangle/x_w)/(\langle S^2 \rangle_\Theta/x_w)_\infty$ against x_w for a-PaMS, where $(\langle S^2 \rangle_\Theta/x_w)_\infty$ denotes the asymptotic value of $\langle S^2 \rangle_\Theta/x_w$ in cyclohexane at 30.5 °C (Θ): (○) present data in toluene at 25.0 °C; (●) present data in 4-*tert*-butyltoluene at 25.0 °C; (◐) present data in *n*-butyl chloride at 25.0 °C; (◑) previous data in cyclohexane at Θ ;⁴ (filled circle with pip up) data in toluene at 25.0 °C by Kato et al.;¹⁰ (filled circle with pip down) data in toluene at 25.0 °C by Kim et al.;²⁴ (filled circle with pip right) data in toluene at 25.0 °C by Kim and Cotts;²⁵ (filled circle with pip left) data in benzene at 30.0 °C by Tsunashima;¹² (◆) data in *n*-butyl chloride at 25.0 °C by Mays et al.²⁶ The upper three solid curves represent the best-fit QTP (or YSS) theory values for the perturbed chain, and the lowest solid curve represents the best-fit HW theory values for the unperturbed chain (see text).

note that the value of S_c^2 in cyclohexane at Θ had been estimated to be 10.7 Å².⁴

The values of $\langle S^2 \rangle^{1/2}$ so determined from SAXS for the a-PaMS samples in toluene at 25.0 °C and in 4-*tert*-butyltoluene at 25.0 °C are given in the fifth and seventh columns, respectively, in the first through ninth rows of Table 2. In the table are also given the values of M_w and $\langle S^2 \rangle^{1/2}$ determined from LS for the a-PaMS samples AMS24 through AMS550 in cyclohexane at Θ , in toluene at 25.0 °C, in 4-*tert*-butyltoluene at 25.0 °C, and in *n*-butyl chloride at 25.0 °C in the 10th through last rows. It is seen from Tables 1 and 2 that the values of M_w determined from LS for each of the samples AMS24 through AMS550 in the four solvents are in good agreement with each other, confirming the accuracy of the LS measurements.

Figure 1 shows double-logarithmic plots of $(\langle S^2 \rangle/x_w)/(\langle S^2 \rangle_\Theta/x_w)_\infty$ against x_w for a-PaMS in the good and Θ

Table 3. Values of α_S^2 of Atactic Oligo- and Poly(α -methylstyrene)s in Good Solvents at 25.0 °C

sample	α_S^2		
	toluene	4- <i>tert</i> -butyltoluene	<i>n</i> -butyl chloride
OAMS8	0.99 ₄		
OAMS10	0.99 ₃		
OAMS13	1.00	0.99 ₁	
OAMS25	1.01		
OAMS33	1.02		
OAMS67	1.08	1.04	
AMS1	1.15		
AMS2	1.26	1.11	
AMS5	1.44		
AMS24	1.86	1.31	1.24
AMS40	2.13	1.39	1.34
AMS80	2.44	1.56	1.42
AMS200	2.80	1.74	1.60
AMS320	3.18	1.96	1.72
AMS550	3.52	2.17	1.83

solvents, where $(\langle S^2 \rangle_\Theta/x_w)_\infty$ denotes the asymptotic value of $\langle S^2 \rangle_\Theta/x_w$ in cyclohexane at Θ in the limit of $x_w \rightarrow \infty$, which had been previously evaluated to be 8.0₅ Å².⁴ The unfilled, bottom-half-filled, and top-half-filled circles represent the values in toluene at 25.0 °C, in 4-*tert*-butyltoluene at 25.0 °C, and in *n*-butyl chloride at 25.0 °C, respectively. The filled circles without pips represent the previous values⁴ and the present one for the sample AMS550 (with the largest x_w) in cyclohexane at Θ . The value of $\langle S^2 \rangle_\Theta/x_w$ for the sample AMS550 is 8.0₂ Å² and is in good agreement with the above-mentioned value 8.0₅ Å² of $(\langle S^2 \rangle_\Theta/x_w)_\infty$, indicating that the difference between the values of f_r (0.70 and 0.72 ± 0.01) of the sample AMS550 and the others has no significant effect on solution properties. In the figure, the upper three solid curves represent the best-fit QTP theory values for the perturbed chain, which are mentioned in the next (Discussion) section, and the lowest solid curve represents the best-fit HW theory values for the unperturbed chain calculated with the values of the model parameters previously determined. (The values of the HW model parameters are also given in Table 4.)

It is seen from Figure 1 that the data in toluene at 25.0 °C and in 4-*tert*-butyltoluene at 25.0 °C agree well with those in cyclohexane at Θ within experimental error in the range of $x_w \lesssim 30$ and then deviate upward progressively from the latter with increasing x_w in the range of $x_w \gtrsim 30$ because of the excluded-volume effect. This agreement in the range of $x_w \lesssim 30$, where the excluded-volume effect may be ignored, enables us to adopt $\langle S^2 \rangle_\Theta$ in cyclohexane at Θ as the unperturbed dimensions $\langle S^2 \rangle_0$ in the good solvents,² toluene at 25.0 °C and 4-*tert*-butyltoluene at 25.0 °C. Although $\langle S^2 \rangle$ in the range of $x_w \lesssim 30$ could not be determined in *n*-butyl chloride at 25.0 °C, we assume that $\langle S^2 \rangle_0$ in it may also be equated to $\langle S^2 \rangle_\Theta$ in cyclohexane at Θ , for convenience. It is also seen from the figure that the excluded volume is the largest in toluene at 25.0 °C and the smallest in *n*-butyl chloride at 25.0 °C.

It is pertinent to make here a remark on the solution temperatures adopted in this paper. In a previous study of α_S of atactic polystyrene (a-PS) with $f_r = 0.59$,²³ the temperature 15.0 °C of solutions in toluene was adopted so that both the values of $\langle S^2 \rangle$ and the intrinsic viscosity of its oligomer with very small x_w in toluene became equal to the corresponding ones in cyclohexane at 34.5 °C (Θ). In the present case of a-PaMS in toluene, however, such a temperature could not be found, so that we adopted the temperature 25.0 °C in toluene at which the coincidence holds only for $\langle S^2 \rangle$. As for solutions in 4-*tert*-butyltoluene and *n*-butyl chloride, we adopted the same temperature as that for solutions in toluene, for convenience.

For comparison, literature data for a-PaMS in good solvents are also plotted in Figure 1 for the samples with $f_r \approx 0.63$ in toluene at 25.0 °C by Kato et al.¹⁰ (filled circles with pip up), those in toluene at 25.0 °C by Kim et al.²⁴ (filled circles with pip down), those in toluene at 25.0 °C by Kim and Cotts²⁵ (filled circles with pip right), those with $f_r \approx 0.68$ in benzene at 30.0 °C by Tsunashima¹² (filled circles with pip left), and those with $f_r \approx 0.74$ in *n*-butyl chloride at 25.0 °C by Mays et al.²⁶ (filled diamonds). The values obtained by Kato et al. are somewhat larger than ours. As noted in the previous paper,⁴ the difference between our and Kato et al.'s values may probably be mainly due to that in f_r . The values obtained by Kim et al. and Kim and Cotts, for which the same commercial samples were used, are scattered around ours and may be considered to agree with ours within experimental error. We note that the values of f_r of their samples, although not reported by them, are considered to be ~ 0.74 . The values obtained by Tsunashima in benzene at 30.0 °C agree with ours in toluene at 25.0 °C within experimental error for $x_w \gtrsim 10^4$. The values obtained by Mays et al. in *n*-butyl chloride at 25.0 °C are appreciably smaller than ours. The reason for this difference is not clear.

Discussion

Excluded-Volume Strength. As shown in the last (Results) section, the unperturbed dimensions $\langle S^2 \rangle_0$ in the three good solvents, toluene at 25.0 °C, 4-*tert*-butyltoluene at 25.0 °C, and *n*-butyl chloride at 25.0 °C, used in this paper may be regarded as equal to $\langle S^2 \rangle_\Theta$ determined experimentally in cyclohexane at 30.5 °C (Θ); that is, $\langle S^2 \rangle_0 = \langle S^2 \rangle_\Theta$. The gyration-radius expansion factor α_S may then be calculated from the defining equation

$$\langle S^2 \rangle = \langle S^2 \rangle_0 \alpha_S^2 \quad (3)$$

with the values of $\langle S^2 \rangle$ given in the fifth, seventh, and ninth (last) columns of Table 2 and those of $\langle S^2 \rangle_\Theta$ given in the third column of Table 2 and Tables 2 and 3 of ref 4. The values of α_S^2 so calculated in the three good solvents are given in Table 3.

Table 4. Values of the HW Model Parameters and the Excluded-Volume Strength for Atactic Poly(α -methylstyrene) and Atactic Polystyrene

polymer (f_r)	solvent	temp, °C	$\lambda^{-1}\kappa_0$	$\lambda^{-1}\tau_0$	λ^{-1} , Å	M_L , Å ⁻¹	λB	β , Å ³
a-PaMS (0.72)	cyclohexane	30.5	3.0	0.9	46.8	39.8	0	0
	toluene	25.0	(3.0)	(0.9)	(46.8)	(39.8)	0.43	36
	4- <i>tert</i> -butyltoluene	25.0	(3.0)	(0.9)	(46.8)	(39.8)	0.12	10
	<i>n</i> -butyl chloride	25.0	(3.0)	(0.9)	(46.8)	(39.8)	0.080	7
a-PS (0.59)	cyclohexane	34.5	3.0	6.0	20.6	35.8	0	0
	toluene	15.0	(3.0)	(6.0)	(20.6)	(35.8)	0.26	33
	4- <i>tert</i> -butyltoluene	50.0	(3.0)	(6.0)	(20.6)	(35.8)	0.10	12

Now, according to the QTP scheme or the Yamakawa–Stockmayer–Shimada (YSS) theory,^{2,27–29} α_S may be given by the Domb–Barrett equation³⁰

$$\alpha_S^2 = [1 + 10\tilde{z} + (70\pi/9 + 10/3)\tilde{z}^2 + 8\pi^{3/2}\tilde{z}^3]^{2/15} \times [0.933 + 0.067 \exp(-0.85\tilde{z} - 1.39\tilde{z}^2)] \quad (4)$$

with the scaled excluded-volume parameter \tilde{z} defined by

$$\tilde{z} = {}^{3/4}_4 K(\lambda L) z \quad (5)$$

in place of the conventional excluded-volume parameter z . The latter is defined by

$$z = (3/2\pi)^{3/2} (\lambda B)(\lambda L)^{1/2} \quad (6)$$

with

$$B = \beta/a^2 c_\infty^{3/2} \quad (7)$$

where β is the binary-cluster integral between beads, a is their spacing (in the touched-bead model), and c_∞ is given by

$$c_\infty = \lim_{\lambda L \rightarrow \infty} (6\lambda \langle S^2 \rangle_0 / L) = \frac{4 + (\lambda^{-1}\tau_0)^2}{4 + (\lambda^{-1}\kappa_0)^2 + (\lambda^{-1}\tau_0)^2} \quad (8)$$

Here, κ_0 and τ_0 are the differential–geometrical curvature κ_0 and torsion τ_0 of the characteristic helix, i.e., the regular helix that the (unperturbed) HW chain takes at the minimum zero of its elastic energy. In eq 5, the coefficient $K(L)$ is given by

$$K(L) = \frac{4}{3} - 2.711L^{-1/2} + \frac{7}{6}L^{-1} \quad \text{for } L > 6$$

$$= L^{-1/2} \exp(-6.611L^{-1} + 0.9198 + 0.03516L) \quad \text{for } L \leq 6 \quad (9)$$

Note that the contour length L is related to the degree of polymerization x by the equation

$$L = xM_0/M_L \quad (10)$$

where M_0 is the molecular weight of the repeat unit and M_L is the shift factor as defined as the molecular weight per unit contour length.

In the QTP scheme, the reduced excluded-volume strength λB may be determined from a comparison of the QTP theory values of α_S^2 with the experimental ones. Figure 2 shows double-logarithmic plots of α_S^2 against x_w for a-PaMS in toluene at 25.0 °C (unfilled circles), in 4-*tert*-butyltoluene at 25.0 °C (bottom-half-filled circles), and in *n*-butyl chloride at 25.0 °C (top-half-filled circles). The solid curves represent the best-fit QTP theory values calculated from eq 4 with eqs 5, 6, 9, and 10 with the values of λ^{-1} and M_L previously⁴ determined, which are given in the sixth and seventh columns, respectively, in the first row of Table 4, and with the values of λB given in the eighth column in the second, third, and fourth rows of Table 4. Note that $M_0 = 118$ for a-PaMS. It is seen that there is good agreement between theory and experiment in each solvent.

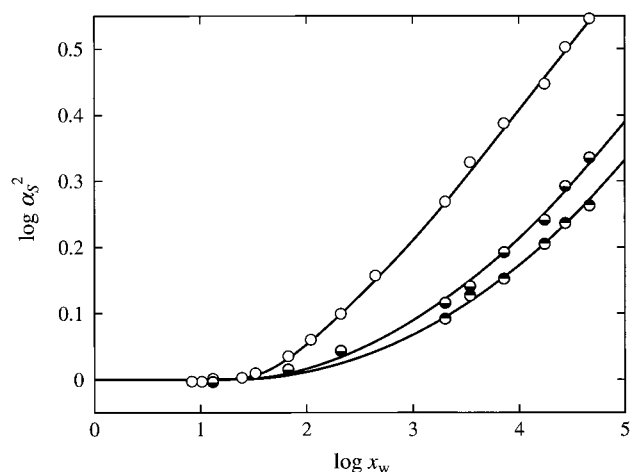


Figure 2. Double-logarithmic plots of α_S^2 against x_w for a-PaMS: (○) in toluene at 25.0 °C; (bottom-half-filled circle) in 4-*tert*-butyltoluene at 25.0 °C; (top-half-filled circle) in *n*-butyl chloride at 25.0 °C. The solid curves represent the QTP (or YSS) theory values (see text).

With the values of λB , we may calculate β from eq 7 with eq 8 with the values of the HW model parameters given in Table 4 and with $a = 2.96$ Å ($=M_0/M_L$). The values of β so calculated are given in the last column in the second, third, and fourth rows of Table 4. For comparison, the values of the HW model parameters, λB , and β for a-PS previously^{2,23,31} determined in cyclohexane at 34.5 °C, in toluene 15.0 °C, and in 4-*tert*-butyltoluene at 50.0 °C are also given in Table 4. It is interesting to see that the values of β itself for a-PaMS are nearly equal to those for a-PS both in toluene and in 4-*tert*-butyltoluene, although the two polymer chains are remarkably different from each other in chain stiffness and local chain conformation. This indicates that the methyl side group in a-PaMS alters the chain stiffness and local chain conformation but has no significant effect on β .

The HW theory value of the perturbed dimension $\langle S^2 \rangle$ may be calculated from eq 3 with α_S^2 given by eq 4 and the HW theory value of the unperturbed dimension $\langle S^2 \rangle_0$ given by²

$$\langle S^2 \rangle_0 = \lambda^{-2} f_S(\lambda L; \lambda^{-1}\kappa_0, \lambda^{-1}\tau_0) \quad (11)$$

where the function f_S is defined by

$$f_S(L; \kappa_0, \tau_0) = \frac{\tau_0^2}{\nu^2} f_{S,KP}(L) + \frac{\kappa_0^2}{\nu^2} \left[\frac{L}{3r} \cos \varphi - \frac{1}{r^2} \cos(2\varphi) + \frac{2}{r^3 L} \cos(3\varphi) - \frac{2}{r^4 L^2} \cos(4\varphi) + \frac{2}{r^4 L^2} e^{-2L} \cos(\nu L + 4\varphi) \right] \quad (12)$$

with

$$\nu = (\kappa_0^2 + \tau_0^2)^{1/2} \quad (13)$$

$$r = (4 + \nu^2)^{1/2} \quad (14)$$

$$\varphi = \cos^{-1}(2/r) \quad (15)$$

and with $f_{S,KP}$ being the function f_S for the Kratky–

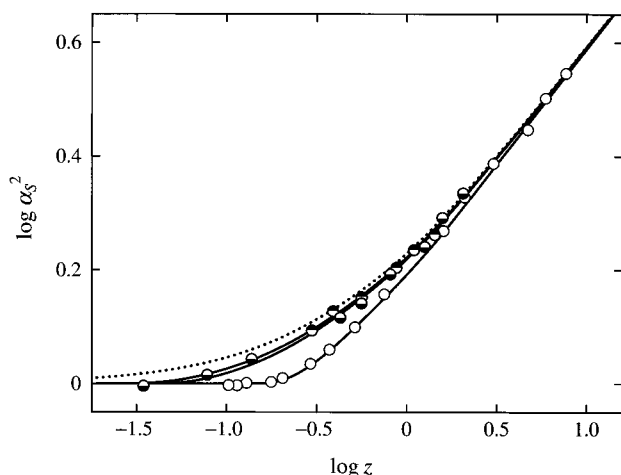


Figure 3. Double-logarithmic plots of α_S^2 against z for a-PaMS. The symbols have the same meaning as those in Figure 2. The solid curves represent the QTP (or YSS) theory values, and the dotted curve represents the corresponding TP theory values (see text).

Porod wormlike chain^{2,32} and being given by

$$f_{S,KP}(L) = \frac{L}{6} - \frac{1}{4} + \frac{1}{4L} - \frac{1}{8L^2}(1 - e^{-2L}) \quad (16)$$

In Figure 1, the upper three solid curves represent the HW theory values so calculated with the values of the parameters given in Table 4.

Validity of the QTP Theory. The same data for α_S^2 as those in Figure 2 are double-logarithmically plotted against z in Figure 3, where values of z have been calculated from eq 6 with eq 10 with the values of λ^{-1} , M_L , and λB given in Table 4. The solid curves represent the QTP theory values calculated from eq 4 with eqs 5 and 6 with the values of λB given in Table 4, and the dotted curve represents the TP theory values calculated from eq 4 with $\tilde{z} = z$. As a natural result of the good agreement between theory and experiment in Figure 2, there is good agreement between them also in Figure 3. It is clearly seen that neither the data points nor the solid curves form a single-composite curve, but both deviate downward progressively from the dotted curve with decreasing z (or M_w) because of the effect of chain stiffness as in the case of the other polymers previously studied (see Figure 8.6 of ref 2). The effect becomes more significant as λB is increased or, in other words, as the solvent quality becomes better. It should be reemphasized that the effect on α_S remains rather large even at $z \approx 10$ or at very large $M_w \approx 10^6$.

Finally, in Figure 4 are shown double-logarithmic plots of α_S^2 against \tilde{z} with the same data as those in Figure 2, where values of \tilde{z} have been calculated from eq 5 with eq 9 with the above values of z . It also includes the values previously determined for a-PS in toluene at 15.0 °C (filled squares),^{2,23} a-PMMA in acetone at 25.0 °C (filled triangles),^{2,33} and isotactic (i-) PMMA with $f_r \approx 0.01$ in acetone at 25.0 °C (inverted filled triangles).^{2,34} The solid curve represents the QTP theory values calculated from eq 4. It is seen that the data points for a-PaMS in the three different good solvents along with those for a-PS and a- and i-PMMA form a single-composite curve. We note that it is natural from the procedure of determining λB that all the present data points for a-PaMS form a single-composite curve and are fitted by the solid curve. The present result together

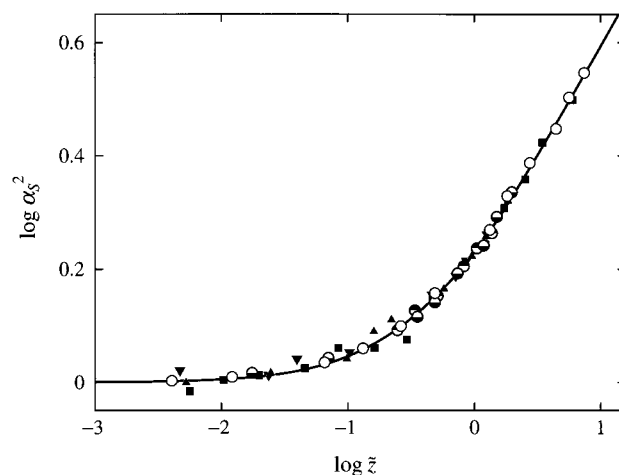


Figure 4. Double-logarithmic plots of α_S^2 against \tilde{z} : (○) a-PaMS in toluene at 25.0 °C; (bottom-half-filled circle) a-PaMS in 4-*tert*-butyltoluene at 25.0 °C; (top-half-filled circle) a-PaMS in *n*-butyl chloride at 25.0 °C; (■) a-PS in toluene at 15.0 °C;²³ (▲) a-PMMA in acetone at 25.0 °C;³³ (▼) i-PMMA in acetone at 25.0 °C.³⁴ The solid curve represents the QTP (or YSS) theory values (see text).

with the good agreement with the data for the other polymers confirms the validity of the QTP prediction that α_S is a function only of \tilde{z} irrespective of the differences in polymer species (chain stiffness and local chain conformation) and solvent condition.

Concluding Remarks

We have made a study of the gyration-radius expansion factor α_S as functions of the conventional excluded-volume parameter z and the scaled excluded-volume parameter \tilde{z} for a-PaMS and its oligomers with $f_r = 0.72$ in the three good solvents: toluene at 25.0 °C, 4-*tert*-butyltoluene at 25.0 °C, and *n*-butyl chloride at 25.0 °C. From a comparison of the present values of $\langle S^2 \rangle$ for the oligomers with the corresponding values of $\langle S^2 \rangle_\Theta$ previously⁴ determined in cyclohexane at 30.5 °C (Θ), it was found that $\langle S^2 \rangle_\Theta$ may be used as the unperturbed dimensions $\langle S^2 \rangle_0$ in those good solvents, so that α_S could be determined from the defining equation $\alpha_S^2 = \langle S^2 \rangle / \langle S^2 \rangle_0 (= \langle S^2 \rangle / \langle S^2 \rangle_\Theta)$. It was shown that the plots of α_S against \tilde{z} so calculated with the parameter values for a-PaMS in the three good solvents along with those for a-PS and a- and i-PMMA form a single-composite curve, confirming the validity of the QTP scheme that all the expansion factors are functions only of \tilde{z} irrespective of the differences in polymer species (chain stiffness and local chain conformation) and solvent condition. We proceed to study the viscosity- and hydrodynamic-radius expansion factors and the second virial coefficient in forthcoming papers.

References and Notes

- (1) Konishi, T.; Yoshizaki, T.; Shimada, J.; Yamakawa, H. *Macromolecules* **1989**, *22*, 1921, and succeeding papers.
- (2) Yamakawa, H. *Helical Wormlike Chains in Polymer Solutions*; Springer: Berlin, 1997.
- (3) Yamakawa, H. *Polym. J.* **1999**, *31*, 109.
- (4) Osa, M.; Yoshizaki, T.; Yamakawa, H. *Macromolecules* **2000**, *33*, 4828.
- (5) Ohgaru, Y.; Sumida, M.; Osa, M.; Yoshizaki, T.; Yamakawa, H. *Macromolecules* **2000**, *33*, 9316.
- (6) Suda, I.; Tominaga, Y.; Osa, M.; Yoshizaki, T.; Yamakawa, H. *Macromolecules* **2000**, *33*, 9322.
- (7) Osa, M.; Sumida, M.; Yoshizaki, T.; Yamakawa, H.; Ute, K.; Kitayama, T.; Hatada, K. *Polym. J.* **2000**, *32*, 361.

- (8) Tamai, Y.; Konishi, T.; Einaga, Y.; Fujii, M.; Yamakawa, H. *Macromolecules* **1990**, *23*, 4067.
- (9) Yoon, D. Y.; Flory, P. J. *Polymer* **1975**, *16*, 645.
- (10) Kato, T.; Miyaso, K.; Noda, I.; Fujimoto, T.; Nagasawa, M. *Macromolecules* **1970**, *3*, 777.
- (11) Noda, I.; Mizutani, K.; Kato, T.; Fujimoto, T.; Nagasawa, M. *Macromolecules* **1970**, *3*, 787.
- (12) Tsunashima, Y. Ph.D. Thesis, Kyoto University, 1972.
- (13) Noda, I.; Mizutani, K.; Kato, T. *Macromolecules* **1977**, *10*, 618.
- (14) Cotts, P. M.; Selser, J. C. *Macromolecules* **1990**, *23*, 2050.
- (15) Hadjichristidis, N.; Lindner, J. S.; Mays, J. W.; Wilson, W. W. *Macromolecules* **1991**, *24*, 6725.
- (16) Li, J.; Harville, S.; Mays, J. W. *Macromolecules* **1997**, *30*, 466.
- (17) Yamakawa, H. *Modern Theory of Polymer Solutions*; Harper & Row: New York, 1971.
- (18) Brownstein, S.; Bywater, S.; Worsfold, D. J. *Makromol. Chem.* **1961**, *48*, 127.
- (19) Deželić, G.; Vavra, J. *Croat. Chem. Acta* **1966**, *38*, 35.
- (20) Berry, G. C. *J. Chem. Phys.* **1966**, *44*, 4550.
- (21) Johnson, B. L.; Smith, J. In *Light Scattering from Polymer Solutions*; Huglin, M. B., Ed.; Academic Press: London, 1972; Chapter 2.
- (22) Konishi, T.; Yoshizaki, T.; Saito, T.; Einaga, Y.; Yamakawa, H. *Macromolecules* **1990**, *23*, 290.
- (23) Abe, F.; Einaga, Y.; Yoshizaki, T.; Yamakawa, H. *Macromolecules* **1993**, *26*, 1884.
- (24) Kim, S. H.; Ramsay, D. J.; Patterson, G. D.; Selser, J. C. *J. Polym. Sci., Polym. Phys.* **1990**, *28*, 2023.
- (25) Kim, S. H.; Cotts, P. M. *J. Appl. Polym. Sci.* **1991**, *42*, 217.
- (26) Mays, J. W.; Nan, S.; Lewis, M. E. *Macromolecules* **1991**, *24*, 4857.
- (27) Yamakawa, H.; Stockmayer, W. H. *J. Chem. Phys.* **1972**, *57*, 2843.
- (28) Yamakawa, H.; Shimada, J. *J. Chem. Phys.* **1985**, *83*, 2607.
- (29) Shimada, J.; Yamakawa, H. *J. Chem. Phys.* **1986**, *85*, 591.
- (30) Domb, C.; Barrett, A. J. *Polymer* **1976**, *17*, 179.
- (31) Arai, T.; Abe, F.; Yoshizaki, T.; Einaga, Y.; Yamakawa, H. *Macromolecules* **1995**, *28*, 3609.
- (32) Kratky, O.; Porod, G. *Recl. Trav. Chim.* **1949**, *68*, 1106.
- (33) Abe, F.; Horita, K.; Einaga, Y.; Yamakawa, H. *Macromolecules* **1994**, *27*, 725.
- (34) Kamijo, M.; Abe, F.; Einaga, Y.; Yamakawa, H. *Macromolecules* **1995**, *28*, 1095.

MA0106550